

Active Zero: Self-Evolving Vision-Language Models through Active Environment Exploration

Jinghan He^{1,2} Junfeng Fang³ Feng Xiong² Zijun Yao⁴ Fei Shen³ Haiyun Guo^{1,2}
Jinqiao Wang^{1,2,5} Tat-Seng Chua³

Abstract

Self-play has enabled large language models to autonomously improve through self-generated challenges. However, existing self-play methods for vision-language models rely on passive interaction with static image collections, resulting in strong dependence on initial datasets and inefficient learning. Without the ability to actively seek visual data tailored to their evolving capabilities, agents waste computational effort on samples that are either trivial or beyond their current skill level. To address these limitations, we propose **Active-Zero**, a framework that shifts from passive interaction to active exploration of visual environments. **Active-Zero** employs three co-evolving agents: a Searcher that retrieves images from open-world repositories based on the model’s capability frontier, a Questioner that synthesizes calibrated reasoning tasks, and a Solver refined through accuracy rewards. This closed loop enables self-scaffolding auto-curricula where the model autonomously constructs its learning trajectory. On Qwen2.5-VL-7B-Instruct across 12 benchmarks, **Active-Zero** achieves 53.97 average accuracy on reasoning tasks (5.7% improvement) and 59.77 on general understanding (3.9% improvement), consistently outperforming existing self-play baselines. These results highlight active exploration as a key ingredient for scalable and adaptive self-evolving vision-language systems.

1. Introduction

Self-play has emerged as a powerful paradigm for agent improvement, where systems bootstrap their capabilities

¹Foundation Model Research Center, Institute of Automation, Chinese Academy of Sciences ²School of Artificial Intelligence, University of Chinese Academy of Sciences ³National University of Singapore ⁴Tsinghua University ⁵Wuhan AI Research. Email: hejinghan2022@ia.ac.cn. Code: <https://github.com/jinghanhe/Active-Zero>.

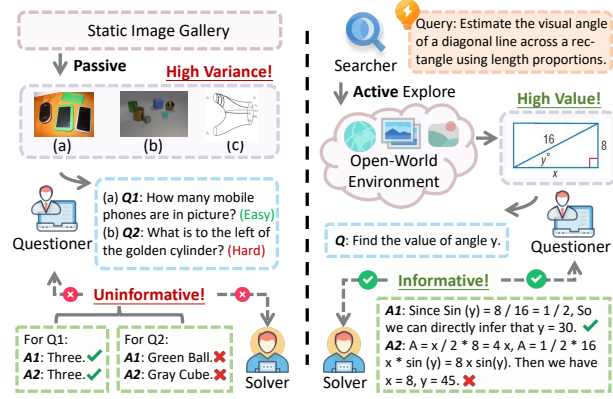


Figure 1. Comparison between Passive Approaches (left) and Active-Zero (right). Unlike traditional methods limited by fixed data boundaries, **Active-Zero** actively explores open-world environments. It employs a Searcher to retrieve high-value images, forming a closed-loop auto-curriculum with the Questioner and Solver to scale VLM reasoning.

by iteratively competing or collaborating with versions of themselves (Gao et al., 2025). Originally demonstrated in game-playing domains (Silver et al., 2018), self-play enables agents to discover novel strategies and transcend their initial training data without human supervision. This principle of autonomous improvement has recently found new application in large language models (LLMs) (Chen et al., 2024b; Wu et al., 2024). Recent work has combined self-play with reinforcement learning with verifiable reward (RLVR) (Lambert et al., 2024), enabling LLMs to self-generate challenging tasks that push the boundaries of their own capabilities. Rather than relying solely on fixed datasets, these models autonomously create reasoning problems, attempt to solve them, and use the outcomes for self-improvement (Zhao et al., 2025; Huang et al., 2025).

Building on this success in language models, self-play is now extending into the multimodal domain, where vision-language models (VLMs) stand to benefit immensely from self-evolution given the vast visual corpora available on the internet (Radford et al., 2021). Despite these advances, the transition from LLMs to VLMs introduces unique complexities: while LLMs operate in a self-contained symbolic space,

VLMs must ground their reasoning in external visual environments (Wang et al., 2025b), requiring careful curation of visual experiences to enable effective self-evolution.

Current approaches address this by employing self-play over pre-collected image sets (He et al., 2025; Thawakar et al., 2025), synthesizing reasoning tasks from static visual galleries. While demonstrating initial promise, these frameworks **operate in a fundamentally passive mode**: they lack the ability to actively curate or explore visual data based on their evolving mastery. As illustrated in Figure 1 (a), this passivity creates two critical bottlenecks. First, it creates a **strong dependency on the initial image collection**—the quality and diversity of self-generated tasks are inherently bounded by the pre-selected visual data, regardless of the model’s growing capabilities. Second, it leads to **learning inefficiency in open-world scenarios**. Without the ability to seek out images tailored to their current capability, agents expend computational effort on samples that are either trivial or beyond their skill level.

To overcome these bottlenecks, we propose a shift from passive interaction with static image galleries to active exploration of open-ended visual environments. As shown in Figure 1 (b), we realize this through **Active-Zero**, a tri-agent framework that closes the loop between data acquisition and reasoning enhancement via a three-stage training protocol. Our approach centers on the iterative optimization of three specialized agents, each addressing a distinct aspect of autonomous evolution. The cycle begins with the **Searcher**, which generates strategic queries to retrieve images from open-world repositories. By optimizing the Searcher to maximize the learning potential of retrieved data, we transform image selection from a static preprocessing step into a dynamic process driven by the model’s evolving capabilities. The **Questioner** then formulates reasoning tasks calibrated to the frontier of the model’s current abilities, ensuring the training signal remains neither trivial nor beyond reach. Finally, the **Solver** is refined via accuracy rewards to deepen its reasoning on these curated challenges. Through this iterative cycle, **Active-Zero** enables a self-scaffolding auto-curriculum where the model autonomously constructs its own learning trajectory, paving the way for more scalable and adaptive VLM reasoning.

We evaluate **Active-Zero** across a comprehensive suite of benchmarks spanning 6 reasoning-intensive tasks and 6 general visual understanding. **Active-Zero** consistently outperforms self-play baselines, demonstrating that active environment exploration enables more effective auto-curriculum learning. On reasoning-intensive benchmarks, **Active-Zero** achieves 53.97 average accuracy on Qwen2.5-VL-7B-Instruct (a 5.7% improvement), surpassing both VisPlay and EvolMM. These gains extend beyond narrow reasoning tasks—on general VLM benchmarks, **Active-Zero**

achieves an average score of 59.77 (+3.9%), compared to 57.51 for the base model. These results demonstrate that by dynamically selecting visual experiences aligned with its evolving capabilities, **Active-Zero** achieves simultaneous gains in both reasoning depth and general visual understanding. Our contributions are summarized as follows:

- We fundamentally shift VLM self-play from passive interaction with static visual data to active exploration of visual environments, enabling agents to dynamically curate training data aligned with their capability frontier.
- We propose **Active-Zero**, a tri-agent framework that co-evolves a Searcher, Questioner, and Solver via iterative optimization, establishing a closed loop between open-world data discovery and reasoning improvement.
- Comprehensive evaluation demonstrates **Active-Zero** outperforms existing self-play baselines on both reasoning and general vision-language benchmarks.

2. Related Work

2.1. Self-Evolving LLMs

Recent work aims to remove the human-data bottleneck by enabling LLMs to self-generate training signals via self-play and verifiable rewards. Absolute Zero couples task proposal and solving in an RLVR loop grounded by executable environments, where tasks are programmatically validated against environment-derived ground truth (Zhao et al., 2025). R-Zero extends this to domains lacking explicit verifiers by replacing external verification with internal self-consistency: a Challenger generates questions targeting 50% Solver agreement, while the Solver trains on difficulty-filtered majority-vote labels, creating an emergent curriculum that tracks the capability frontier (Huang et al., 2025). Beyond zero-data regimes, grounded self-play leverages external corpora to provide novelty and anchoring. SPELL enables long-context reasoning by cycling through questioner, responder, verifier roles, using semantic-equivalence verification and progressive length curricula for continual improvement (Yang et al., 2025). SPICE generates question-answer pairs from documents, training a reasoner with variance-shaped rewards that track the capability frontier (Liu et al., 2025b). Complementary directions include self-rewarding frameworks that bootstrap RL from limited supervision (Fang et al., 2025), game-theoretic alignment via iterative self-play (Wu et al., 2024), and curriculum-centric post-training that optimizes task selection for reasoning improvement (Chen et al., 2025b).

2.2. Active Data Curation

Active data curation differs from conventional subset selection in that the learner acts to decide what data to obtain next,

rather than sampling from a fixed pool. In vision-language settings, active learning variants select images or prompts using model-conditioned signals such as uncertainty or neighborhood structure to maximize improvement per labeled example (Safaei & Patel, 2025; Udandarao et al., 2025). Closer to open-world acquisition, target-driven dataset acquisition cast data collection as a planned process where an agent generates queries to retrieve task-suitable training data from external repositories (Berkane et al., 2025). A complementary direction studies adaptive curricula that reorder or schedule training data according to model-dependent difficulty, emphasizing that useful data changes as the model evolves (Zhang et al., 2025). Our work aligns with the active side of this literature: rather than reweighting a static dataset, **Active-Zero** optimizes a Searcher to acquire challenging visual data from open-world repositories, then integrates acquisition with task synthesis and solving to form a closed-loop curriculum.

2.3. Self-Evolving LVLMs

Self-evolving LVLMs extend LLM self-play to visually grounded settings by generating tasks and rewards over images. VisPlay performs self-play on unlabeled images by co-training an image-conditioned Questioner and Reasoner with RL updates and difficulty-diversity shaping (He et al., 2025). EvoLMM advances a similar Proposer–Solver loop but emphasizes continuous self-reward through consistency-based signals to drive improvement without external supervision (Thawakar et al., 2025). Vision-zero reframes multimodal self-improvement as strategic, gamified self-play to better control task difficulty and mitigate plateaus (Wang et al., 2025a). Moving toward co-adaptation, C2-Evo explicitly co-evolves multimodal data complexity and model capability in a closed loop, targeting reasoning domains like multimodal math and geometry (Chen et al., 2025a). While these methods demonstrate the viability of self-play for VLMs, they operate over static image collections, treating the visual environment as fixed. In contrast, **Active-Zero** introduces active environment exploration: a learned Searcher dynamically retrieves images from open-world repositories based on the model’s evolving capabilities, transforming the training environment into a controllable variable.

3. Method

3.1. Preliminary

Group Relative Policy Optimization (GRPO) (Shao et al., 2024) is an efficient reinforcement learning algorithm that optimizes models by eliminating the need for a separate value-function critic. For each input q , the old policy $\pi_{\theta_{old}}$ generates a group of G independent responses $\{o_i\}_{i=1}^G$, where $o_i = \{o_{i,1}, \dots, o_{i,T_i}\}$ is a token sequence. Each response o_i receives a reward r_i . The policy π_θ is updated

with a clipped objective at each token step t :

$$\mathcal{L}_{i,t}^{clip}(\theta) = \min \left(r_{i,t}(\theta) \hat{A}_i, \text{clip}(r_{i,t}(\theta), \epsilon_{low}, \epsilon_{high}) \hat{A}_i \right), \quad (1)$$

where the importance ratio $r_{i,t}(\theta)$ and the advantage \hat{A}_i are:

$$r_{i,t}(\theta) = \frac{\pi_\theta(o_{i,t}|q, o_{i,<t})}{\pi_{\theta_{old}}(o_{i,t}|q, o_{i,<t})}, \quad \hat{A}_i = \frac{r_i - \text{mean}(\{r_k\}_{k=1}^G)}{\text{std}(\{r_k\}_{k=1}^G)}. \quad (2)$$

In our framework, all three specialized agents are iteratively optimized using this mechanism to identify and bridge reasoning gaps.

3.2. Framework Overview

We introduce **Active-Zero**, a self-play framework that automates the evolution of visual reasoning in VLMs through active environment exploration. Unlike passive approaches that rely on static image collections, **Active-Zero** actively explores open-world visual environments to construct its own training curriculum. The system comprises three specialized agents—the **Searcher** (\mathcal{S}), **Questioner** (\mathcal{Q}), and **Solver** (\mathcal{V})—all initialized from a single base model but optimized for distinct roles. As illustrated in Figure 2, the framework operates through a co-evolutionary cycle partitioned into three synergistic stages:

- **Active Environment Exploration (Stage 1):** \mathcal{S} navigates an expansive visual environment \mathcal{D}_{env} to retrieve images at the edge of the Solver’s current capabilities—scenarios where the Solver is uncertain but not overwhelmed, ensuring high informational value.
- **Adaptive Task Synthesis (Stage 2):** \mathcal{Q} transforms retrieved images into complex, multi-step reasoning questions x calibrated to maximize the Solver’s uncertainty, converting visual contexts into instructional curricula.
- **Reasoning Optimization (Stage 3):** \mathcal{V} is optimized on the synthesized curriculum \mathcal{D}_{train} , through consensus-based reinforcement learning, bridging current reasoning gaps and raising the bar for subsequent iterations.

All three agents are optimized using GRPO, which employs a group-based advantage mechanism to filter noise and promote self-consistent reasoning trajectories. This unified RL backbone enables **Active-Zero** to autonomously scale reasoning complexity without exhaustive human annotation.

3.3. Stage 1: Active Environment Exploration

The Searcher \mathcal{S} identifies visual scenarios that expose the Solver’s current limitations. Formally, \mathcal{S} is a policy $\pi_{\mathcal{S}}(q|P)$ that generates semantic retrieval queries q conditioned on a domain-specific prompt P . Each query interacts with a retrieval function to fetch an image $I = \text{Ret}(q, \mathcal{D}_{env})$.

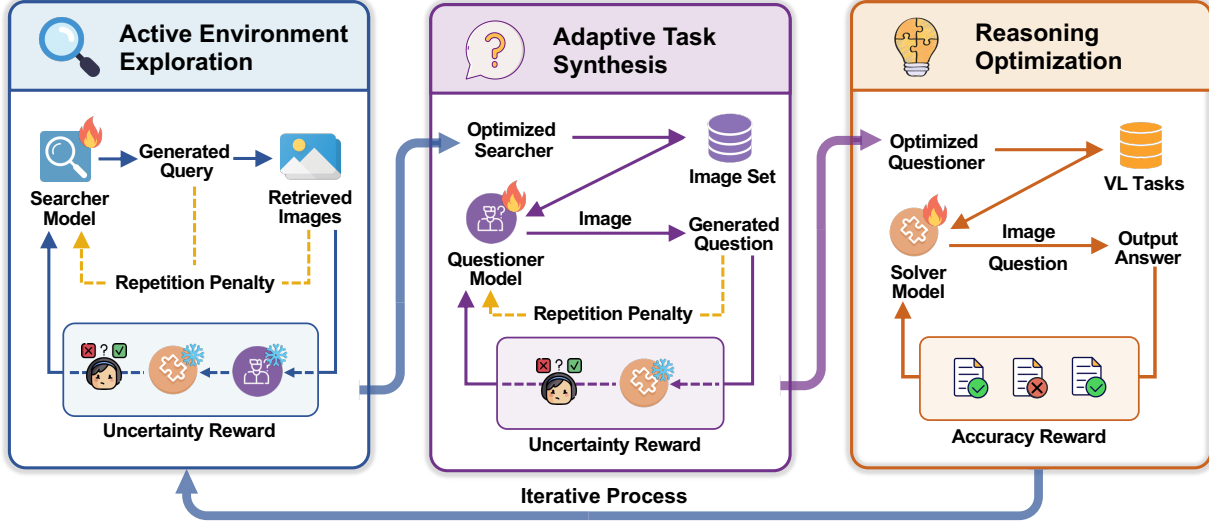


Figure 2. Overview of the Active-Zero framework. The system facilitates an iterative, three-stage self-play cycle to enhance VLM reasoning: **(Stage 1)** The **Searcher** (\mathcal{S}) is optimized to retrieve informative images from the environment by balancing a challenge reward (targeting the Solver’s uncertainty) and a repetition penalty. **(Stage 2)** The **Questioner** (\mathcal{Q}) synthesizes complex, multi-step questions from the curated images to maximize instructional utility. **(Stage 3)** The **Solver** (\mathcal{V}) is trained on the generated tasks to improve reasoning accuracy and consensus via reinforcement learning. The entire process is iterative, allowing the agents to co-evolve as the Solver’s capability frontier shifts.

Reward Formulation. To prioritize informative samples, we optimize \mathcal{S} toward the frontier of the Solver’s capabilities. Following (Huang et al., 2025), we define a challenge reward R_{chal} based on the Solver’s predictive uncertainty. For a retrieved image I , we sample a probe question $x \sim \mathcal{Q}(\cdot|I)$ and execute m independent reasoning passes through \mathcal{V} to obtain an answer set $\{y_1, \dots, y_m\}$. The Solver’s empirical accuracy is then computed as:

$$\text{Acc}(\mathcal{V}, I, x) = \frac{1}{m} \sum_{j=1}^m \mathbb{I}[y_j = \hat{y}], \quad (3)$$

where \hat{y} denotes the majority-voted consensus. The challenge reward peaks at maximum uncertainty:

$$R_{chal}(q) = \mathbb{E}x \sim \mathcal{Q}(\cdot|I) \left[1 - 2 \left| \text{Acc}(\mathcal{V}, I, x) - \frac{1}{2} \right| \right]. \quad (4)$$

Maximizing R_{chal} compels the Searcher to identify visual contexts at the Solver’s capability frontier—tasks just beyond its deterministic grasp yet within its latent reasoning potential.

Diversity Control. To prevent the policy from converging on narrow query sets, we implement a dual-modality repetition penalty \mathcal{P}_{rep} . For each batch $\mathbf{Q} = \{q_i\}_{i=1}^n$ with retrieved images $\mathbf{I} = \{I_i\}_{i=1}^n$, we quantify pairwise similar-

ity in both text and visual spaces.

$$\begin{aligned} d_{ij}^{txt} &= 1 - \text{BLEU}(q_i, q_j), \\ d_{ij}^{vis} &= 1 - \cos(\phi(I_i), \phi(I_j)), \end{aligned} \quad (5)$$

where $\phi(\cdot)$ represents a frozen image encoder. We cluster a batch of samples into \mathcal{C}^{txt} and \mathcal{C}^{vis} based on sensitivity thresholds τ_{txt} and τ_{vis} . The penalty for query-image pair (q_i, I_i) is then proportional to neighborhood density:

$$\mathcal{P}_{rep}(q_i, I_i) = \frac{|\mathcal{C}^{txt}(q_i)|}{n} + \frac{|\mathcal{C}^{vis}(I_i)|}{n}. \quad (6)$$

The final reward is $R_{\mathcal{S}} = \max(0, R_{chal} - \mathcal{P}_{rep})$, encouraging the agent to explore diverse coordinates across the visual-semantic manifold.

Domain-Conditioned Exploration. To maintain a balanced curriculum across heterogeneous tasks, we partition the search space into N semantic domains: $\mathcal{C} = \{c_1, c_2, \dots, c_N\}$. Each domain is governed by a specialized prompt template P_c that constrains $\pi_{\mathcal{S}}$ to relevant visual-logical properties. To prevent the model from ignoring challenging domains in favor of easier ones with higher absolute rewards, we utilize the group-relative nature of GRPO. For a group of G queries within domain c , the advantage \hat{A} is normalized strictly against domain-specific peers:

$$\hat{A}(q_{i,c}) = \frac{R_{\mathcal{S}}(q_{i,c}) - \mu_c}{\sigma_c}. \quad (7)$$

This ensures that the Searcher seeks the most informative data within every domain, sustaining a robust auto-curriculum across the multi-modal spectrum.

3.4. Stage 2: Adaptive Task Synthesis

Following optimization of the search policy, we deploy π_S^* to curate an active visual dataset $\mathcal{D}_{active} = \{I_j\}_{j=1}^M$. The Questioner $\pi_Q(x|I, T_{cot})$ synthesizes complex reasoning tasks x from these images. We employ a Chain-of-Thought (CoT) template T_{cot} to guide the Questioner to deconstruct visual-logical constraints prior to question formulation.

Reward Formulation. Similar to the Searcher, the Questioner aims to maximize the instructional utility of the generated questions by targeting the Solver’s current weaknesses. The reward R_Q for question x_i generated from image I is:

$$R_Q(x_i) = \max(0, R_{chal}(x_i|I) - \mathcal{P}_{rep}(x_i)), \quad (8)$$

where $R_{chal}(x_i|I)$ is the challenge reward from Equation (4) for question x_i , and \mathcal{P}_{rep} is a linguistic repetition penalty preventing collapse into repetitive question structures.

By maximizing R_{chal} , the Questioner generates tasks that avoid both trivial consensus and complete randomness, creating a curriculum that bridges the Solver’s current state and higher-order reasoning capabilities.

3.5. Stage 3: Reasoning Optimization

Training Set Construction. In the final stage, we deploy the optimized policy π_Q^* over \mathcal{D}_{active} to construct an initial training pool $\mathcal{D}_{train} = \{(I_j, x_j)\}_{j=1}^M$. For each task, we compute a silver-standard consensus answer \hat{a} by majority vote over K sampled reasoning trajectories from π_V . To focus on informative samples, we filter the pool to retain tasks where empirical accuracy $Acc(\mathcal{V}, I, x)$ falls within difficulty window $(\tau_{low}, \tau_{high})$, yielding curated subset \mathcal{D}_{train}^* . This ensures the Solver optimize trajectories that are neither trivially solved nor beyond its current capacity.

Reward Formulation. The Solver is optimized via GRPO to maximize the accuracy reward signal against pseudo-labels. For each task $(I, x) \in \mathcal{D}_{train}^*$, we sample a group of G independent reasoning trajectories $\{\tau_1, \dots, \tau_G\}$, where each τ_i consists of a CoT path and final answer a_i . The reward for a trajectory τ_i is defined as:

$$R_V(\tau_i) = \begin{cases} 1, & \text{if } a_i = \hat{a}, \\ 0, & \text{otherwise.} \end{cases} \quad (9)$$

This process ultimately enhances the Solver’s ability to navigate the complex visual reasoning challenges synthesized by the preceding agents.

4. Experiments

4.1. Implementation Details

Visual Environment Setup. To facilitate efficient and reproducible training, we construct a diverse visual environment \mathcal{D}_{env} by aggregating the image from The Cauldron (Laurençon et al., 2024), a comprehensive collection of 50 vision-language datasets, and three geometry-focused datasets: Geo3K (Lu et al., 2021), UniGeo (Chen et al., 2022), and GeoQA+ (Cao & Xiao, 2022). The resulting \mathcal{D}_{env} contains 1.6M images, providing a controlled testbed for analyzing the Searcher’s behavior and while ensuring reproducibility without the temporal stochasticity and latency of real-time web APIs.

Retrieval Infrastructure. The Searcher \mathcal{S} interfaces with the environment via a vector retrieval system. We use SigLIP-2 (Tschanne et al., 2025) to generate visual embeddings for all images in \mathcal{D}_{env} , indexed using FAISS (Douze et al., 2025) for sub-millisecond search. When the Searcher generates query q , the retrieval function $Ret(q, \mathcal{D}_{env})$ computes the cosine similarity between the query embedding and the visual index to return the top-k candidate.

System Scalability. While our implementation operates on this pre-indexed local structure for computational efficiency, the Searcher’s query-based interface is backend-agnostic. This architecture enables seamless transition to real-time web exploration or specialized domain-specific databases by swapping the retrieval backend. The million-level local repository provides sufficient diversity to challenge the Searcher’s discovery capabilities while maintaining stability required for iterative optimization.

Optimization Hyperparameters. All three agents are optimized using GRPO (Shao et al., 2024) with a group size of $G = 8$. Clustering thresholds are $\tau_{txt} = 0.5$ and $\tau_{vis} = 0.1$. To construct \mathcal{D}_{active} , we sample 6000 queries from π_S and retrieve the top 5 images per query from \mathcal{D}_{env} , followed by a deduplication. For each image in \mathcal{D}_{active} , one question is generated from π_Q to form \mathcal{D}_{train} . The difficulty filtering thresholds are $\tau_{low} = 0.3$ and $\tau_{high} = 0.8$. Training is conducted on 16 NVIDIA H20 GPUs using the EasyR1 library (Zheng et al., 2025). Additional Details are in Section A.

Evaluation Protocol. We use a consistent CoT prompt for all models and report greedy decoding results. Predefined format-matching rules are used to extract final answers from model responses. To avoid limitations of rigid string matching, we use DeepSeek-V3.2 (Liu et al., 2025a) as an automated evaluator. The LLM receives the question, ground truth, and extracted answer to judge semantic and logical consistency, ensuring that correct reasoning is not penalized for formatting variations. We provide the benchmark details in Section A and evaluation prompts in Section B.

Table 1. Comparison of Active-Zero against state-of-the-art baselines on reasoning-intensive benchmarks.

Method	MathVista	MathVision	WeMath	MathVerse	LogicVista	DynaMath	Average
<i>Qwen2.5-VL-3B-Instruct</i>							
Base Model	57.80	22.27	53.51	30.84	37.28	46.33	41.34
VisPlay	58.10 <small>+0.30</small>	22.43 <small>+0.16</small>	58.16 <small>+4.65</small>	34.58 <small>+3.74</small>	39.29 <small>+2.01</small>	50.02 <small>+3.69</small>	43.76 <small>+2.42</small>
Active-Zero	60.20 <small>+2.40</small>	23.62 <small>+1.35</small>	61.21 <small>+7.70</small>	35.09 <small>+4.25</small>	40.62 <small>+3.34</small>	51.24 <small>+4.91</small>	45.33 <small>+3.99</small>
<i>Qwen2.5-VL-7B-Instruct</i>							
Base Model	69.40	25.95	64.48	45.11	43.08	58.26	51.05
VisionZero-CLEVR	70.20 <small>+0.80</small>	24.67 <small>-1.28</small>	66.90 <small>+2.42</small>	45.05 <small>-0.06</small>	41.29 <small>-1.79</small>	58.70 <small>+0.44</small>	51.14 <small>+0.09</small>
VisionZero-Chart	68.20 <small>-1.20</small>	25.16 <small>-0.79</small>	64.66 <small>+0.18</small>	46.57 <small>+1.46</small>	46.21 <small>+3.13</small>	58.40 <small>+0.14</small>	51.53 <small>+0.48</small>
VisionZero-RealWorld	69.20 <small>-0.20</small>	26.12 <small>+0.17</small>	65.40 <small>+0.92</small>	45.62 <small>+0.51</small>	48.44 <small>+5.36</small>	58.62 <small>+0.36</small>	52.23 <small>+1.18</small>
VisPlay	69.40 <small>+0.00</small>	27.04 <small>+1.09</small>	67.99 <small>+3.51</small>	43.59 <small>-1.52</small>	45.09 <small>+2.01</small>	58.98 <small>+0.72</small>	52.02 <small>+0.97</small>
EvoLMM	69.80 <small>+0.40</small>	24.11 <small>-1.84</small>	64.89 <small>+0.41</small>	44.80 <small>-0.31</small>	46.65 <small>+3.57</small>	58.06 <small>-0.20</small>	51.39 <small>+0.34</small>
Active-Zero	72.60 <small>+3.20</small>	26.18 <small>+0.23</small>	69.60 <small>+5.12</small>	48.16 <small>+3.05</small>	48.21 <small>+5.13</small>	59.04 <small>+0.78</small>	53.97 <small>+2.92</small>

Table 2. Comparison of Active-Zero against state-of-the-art baselines on general visual understanding and knowledge-based benchmarks.

Method	VisNum	RealWorld	MMStar	MMMU	MMMU.Pro	Hallusion	Average
<i>Qwen2.5-VL-3B-Instruct</i>							
Base Model	34.71	61.70	52.80	44.69	41.99	60.04	49.32
VisPlay	37.32 <small>+2.61</small>	59.48 <small>-2.22</small>	51.60 <small>-1.20</small>	44.80 <small>+0.11</small>	42.43 <small>+0.44</small>	64.88 <small>+4.84</small>	50.09 <small>+0.77</small>
Active-Zero	41.51 <small>+6.80</small>	60.00 <small>-1.70</small>	53.80 <small>+1.00</small>	49.16 <small>+4.47</small>	46.70 <small>+4.71</small>	64.14 <small>+4.10</small>	52.55 <small>+3.23</small>
<i>Qwen2.5-VL-7B-Instruct</i>							
Base Model	44.85	63.66	61.53	53.52	52.61	68.87	57.51
VisionZero-CLEVR	43.13 <small>-1.72</small>	66.41 <small>+2.75</small>	62.07 <small>+0.54</small>	56.98 <small>+3.46</small>	52.17 <small>-0.44</small>	69.51 <small>+0.64</small>	58.38 <small>+0.87</small>
VisionZero-Chart	44.54 <small>-0.31</small>	64.05 <small>+0.39</small>	62.27 <small>+0.74</small>	53.07 <small>-0.45</small>	51.67 <small>-0.94</small>	69.09 <small>+0.22</small>	57.45 <small>-0.06</small>
VisionZero-RealWorld	44.17 <small>-0.68</small>	65.36 <small>+1.70</small>	62.27 <small>+0.74</small>	53.30 <small>-0.22</small>	52.29 <small>-0.32</small>	68.56 <small>-0.31</small>	57.66 <small>+0.15</small>
VisPlay	45.22 <small>+0.37</small>	63.27 <small>-0.39</small>	62.93 <small>+1.40</small>	52.51 <small>-1.01</small>	51.98 <small>-0.63</small>	68.56 <small>-0.31</small>	57.41 <small>-0.10</small>
EvoLMM	45.01 <small>+0.16</small>	61.44 <small>-2.22</small>	61.53 <small>+0.00</small>	55.31 <small>+1.79</small>	51.60 <small>-1.01</small>	69.72 <small>+0.85</small>	57.44 <small>-0.07</small>
Active-Zero	47.94 <small>+3.09</small>	67.58 <small>+3.92</small>	64.00 <small>+2.47</small>	56.42 <small>+2.90</small>	54.62 <small>+2.01</small>	68.03 <small>-0.84</small>	59.77 <small>+2.26</small>

Table 3. Ablation study on Active-Zero components.

Method	Reasoning Avg.	General Avg
Active-Zero	45.33	52.55
<i>Searcher Effectiveness</i>		
↪ Base Searcher	44.75 <small>-0.58</small>	51.03 <small>-1.52</small>
↪ Random Sampling	43.88 <small>-1.45</small>	51.86 <small>-0.69</small>
<i>Ablations</i>		
↪ w/o Domain-Conditioned	44.93 <small>-0.40</small>	50.73 <small>-1.82</small>
↪ w/o Visual Penalty	44.89 <small>-0.44</small>	51.62 <small>-0.93</small>

4.2. Main Results

We evaluate Active-Zero across a comprehensive suite of benchmarks. As shown in Tables 1 and 2, we compare our framework against the Base Model and recent self-play baselines, including VisionZero (Wang et al., 2025a), VisPlay (He et al., 2025), and EvolMM (Thawakar et al., 2025).

Reasoning-Intensive Benchmarks. As shown in Table 1, Active-Zero delivers the strongest overall results at both model scales. It raises the average score on Qwen2.5-VL-3B-Instruct from 41.34 to 45.33 (+3.99) and on Qwen2.5-

VL-7B-Instruct from 51.05 to 53.97 (+2.92). Improvements are consistent across all six benchmarks. For the 7B model, the largest gains come from LogicVista (48.21 vs. 43.08) and WeMath (69.60 vs. 64.48). Notably, Active-Zero also outperforms all prior self-play methods on the 7B setting, reaching a 53.97 average versus 52.02 for VisPlay and 51.39 for EvolMM, highlighting the benefit of uncertainty-driven retrieval and task synthesis over existing curricula.

General Visual Understanding. In Table 2, Active-Zero also improves general VLM performance, reaching the best average on Qwen2.5-VL-7B-Instruct (59.77 vs. 57.51 for the base model). Improvements are consistent across VisNum, RealWorldQA, MMStar, MMMU, and MMMU-Pro (e.g., 47.94 on VisNum and 67.58 on RealWorldQA), while Hallusion remains comparable but slightly lower than the base model (68.03 vs. 68.87). On Qwen2.5-VL-3B-Instruct, Active-Zero similarly increases the average from 49.32 to 52.55, with particularly strong performance on VisNum (41.51) and MMMU-Pro (46.70).

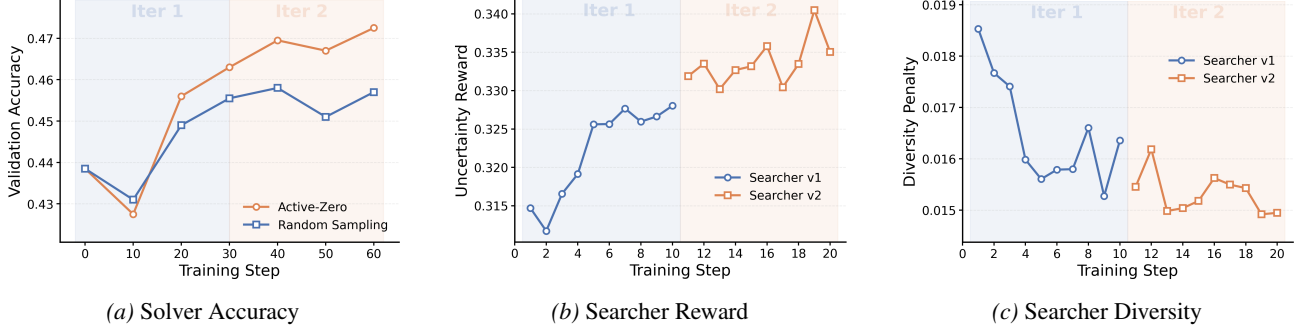


Figure 3. **Co-evolution of Solver and Searcher.** Active-Zero shows superior accuracy scaling in (a), driven by the Searcher’s ability to maximize uncertainty (b) while maintaining high sample diversity (c) through RL-based optimization.

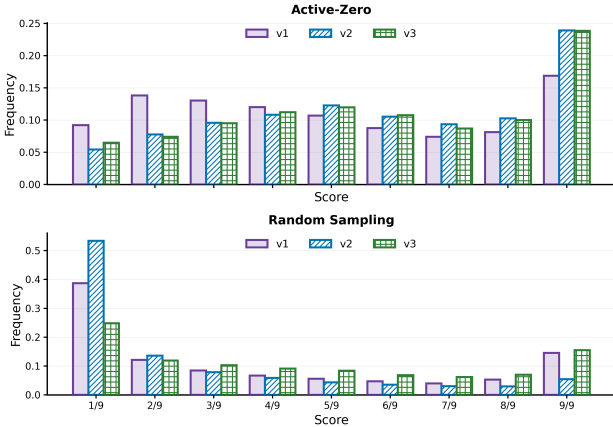


Figure 4. **Consensus-score distribution of generated VL tasks** under Active-Zero and Random Sampling across training versions (v1–v3). The consensus score measures agreement among multiple Solver rollouts on the same question.

4.3. Effectiveness of Active Environment Exploration

We study the contribution of the Searcher \mathcal{S} using the 3B setting as a controlled baseline (Table 3).

Searcher vs. Random Sampling. Replacing Active-Zero with random image retrieval reduces the reasoning average from 45.33 to 43.88. This drop (1.45 points) indicates that actively selecting informative samples is substantially more effective than uniform sampling from \mathcal{D}_{env} for improving reasoning. A similar degradation is observed in general performance (52.55 \rightarrow 51.86), suggesting that informed retrieval benefits both reasoning-specific and broader visual understanding objectives.

Effect of RL Optimization. Disabling RL optimization in the Searcher leads to a consistent degradation, with reasoning dropping to 44.75 and general performance to 51.03. Compared to the full method (45.33 / 52.55), this suggests that RL-based selection better matches the Solver’s learning needs than heuristic or unoptimized retrieval. Notably, the random variant attains a higher general average (51.86) than

the unoptimized Searcher (51.03), implying that without RL, the Searcher may over-focus on samples that benefit reasoning at the expense of broad coverage.

4.4. Ablation Study

We further validate two key design choices in the lower section of Table 3.

Domain-Conditioned Exploration. Removing domain conditioning decreases both reasoning (45.33 \rightarrow 44.93) and general performance (52.55 \rightarrow 50.73). The larger drop on general benchmarks suggests that domain-aware partitioning helps maintain a balanced curriculum across heterogeneous domains, preventing skewed exploration.

Visual Redundancy Control. We ablate the visual repetition penalty \mathcal{P}_{rep} while keeping other components unchanged. Removing it reduces the reasoning average to 44.89 and the general average to 51.62. This supports the role of visual diversity control in preventing the Searcher from repeatedly sampling near-duplicate images, thereby improving coverage of the visual-semantic space needed for robust reasoning.

4.5. Training Dynamics

To better understand the self-play process, we visualize the co-evolution of the Solver, the Searcher, and the reward signals during training in Figure 3.

Solver evolution and the benefit of active sampling. In Figure 3a, Active-Zero consistently achieves higher validation accuracy than the random-retrieval baseline, with the gap becoming more apparent in later training steps. This trend suggests that uncertainty-driven sample selection provides a stronger curriculum than uniform sampling, especially as the Solver becomes capable of benefiting from harder but still learnable examples.

Searcher learning signal across phases. Figure 3b shows that the uncertainty reward rises across both training phases

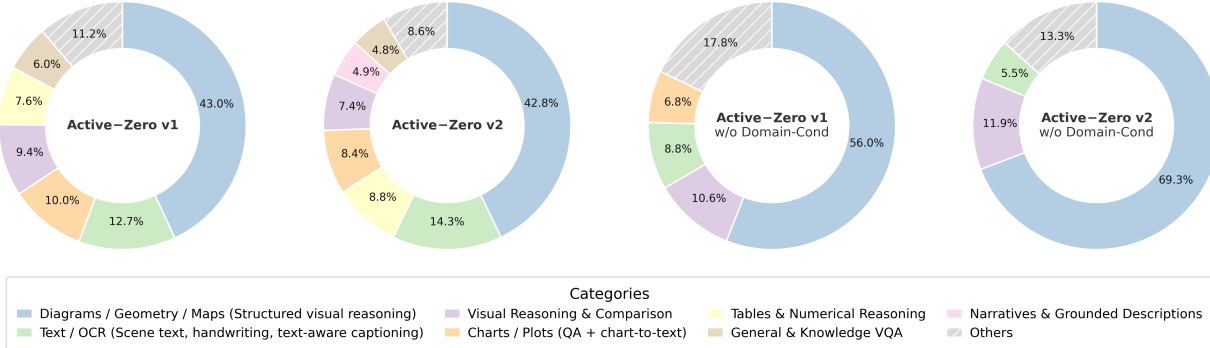


Figure 5. Category distribution of Searcher-retrieved images. Pie charts show the percentage of retrieved images in each task category for Active-Zero v1 and v2, with (left) and without (right) domain conditioning. Categories are identified based on source datasets in \mathcal{D}_{env} .

(v1 and v2), suggesting the Searcher increasingly retrieves examples informative for the current Solver. Meanwhile, Figure 3c shows the diversity penalty drops early and then stabilizes, indicating the Searcher avoids collapsing onto near-duplicate high-uncertainty images. Overall, it maintains broad coverage while improving the reward signal, balancing informativeness and diversity.

4.6. Discussion

Active exploration yields healthier difficulty distribution.

To diagnose how exploration reshapes the curriculum, we analyze the consensus distribution of generated questions in Figure 4. The consensus score measures agreement among multiple Solver rollouts. Low consensus indicates unstable or overly difficult questions, high consensus reflects reliably solved questions, and intermediate consensus corresponds to moderately challenging samples near the Solver’s capability frontier. Compared to Random Sampling, **Active-Zero** shifts mass away from the lowest-consensus bin and increases mid-to-high consensus questions across versions (v1–v3). Random Sampling concentrates heavily in the minimum-consensus bin, indicating that uniform retrieval often produces noisy or weakly grounded questions with inconsistent training signals. This validates that active retrieval better supports coherent, learnable questions.

Active exploration yields naturally diverse curricula. As illustrated in Figure 5, **Active-Zero** Searcher distributes retrievals across diverse task categories: Diagrams/Geometry (43%), Text/OCR (12.7–14.3%), Visual Reasoning (9.4–11.9%), and multiple others, demonstrating that active retrieval naturally discovers varied visual reasoning challenges. Domain-conditioned exploration (left) further stabilizes this balance, while its removal (right) causes gradual concentration toward easier categories, validating the robustness of the active exploration framework.

Query evolution reflects adaptive curriculum construction. We analyze how the Searcher’s retrieval strategy



Figure 6. Query Distribution Shift Across Searcher Versions. Word clouds visualizing the query tokens with increased frequency from Searcher v1 to v2. Larger font sizes indicate larger relative frequency gains.

evolves by tracking query token frequency changes across training versions (Figure 6). From v1 to v2, the Searcher progressively adopts more structural and process-oriented vocabulary, with increased use of terms like *field*, *direction*, *diagram*, *forces*, *folded*, *magnetic*. This shift indicates movement from generic visual descriptors toward images encoding spatial relationships, physical properties, and multi-component structures that demand integrative reasoning. The emergence of technical and relational terminology suggests the Searcher adapts queries in response to the Solver’s learning progress, increasingly targeting images with richer structural information. This qualitative evolution aligns with the consensus analysis in Figure 4, where active exploration reduces unstable samples and concentrates toward more learnable questions at the Solver’s capability frontier, demonstrating that the framework constructs increasingly sophisticated curricula as training progresses.

5. Conclusion

We presented **Active-Zero**, a self-play framework that re-thinks how vision-language models improve in open-world settings. Rather than passively training on static image collections, **Active-Zero** enables models to actively explore visual environments and autonomously construct curricula aligned with their evolving capabilities. By closing the

loop between data acquisition, task generation, and reasoning optimization, the proposed Searcher–Questioner–Solver tri-agent system transforms self-play into a dynamic, self-scaffolding learning process. Extensive experiments across 12 benchmarks demonstrate that active environment exploration leads to consistent and complementary gains in both reasoning-intensive tasks and general visual understanding, paving the way for more adaptive VLM reasoning.

Impact Statement

This paper advances vision-language model reasoning through self-play and active exploration. The primary benefit is enabling more capable multimodal AI systems that can autonomously improve without extensive human annotation, potentially democratizing access to high-quality models.

We acknowledge potential risks: active exploration systems querying open-world repositories could inadvertently amplify biases or access inappropriate content, and self-improvement without human oversight raises alignment concerns. While our implementation uses curated datasets, future deployments to live web retrieval would require content filtering, bias mitigation, and safety guardrails. We encourage practitioners to implement appropriate oversight mechanisms when adopting active exploration paradigms.

References

Bai, S., Chen, K., Liu, X., Wang, J., Ge, W., Song, S., Dang, K., Wang, P., Wang, S., Tang, J., et al. Qwen2. 5-vl technical report. *arXiv preprint arXiv:2502.13923*, 2025.

Berkane, T., Charpignon, M.-L., and Majumder, M. S. LLM-based web data collection for research dataset creation. In Christodoulopoulos, C., Chakraborty, T., Rose, C., and Peng, V. (eds.), *Findings of the Association for Computational Linguistics: EMNLP 2025*, pp. 12610–12622, Suzhou, China, November 2025. Association for Computational Linguistics. ISBN 979-8-89176-335-7. doi: 10.18653/v1/2025.findings-emnlp.674. URL <https://aclanthology.org/2025.findings-emnlp.674/>.

Cao, J. and Xiao, J. An augmented benchmark dataset for geometric question answering through dual parallel text encoding. In Calzolari, N., Huang, C.-R., Kim, H., Pustejovsky, J., Wanner, L., Choi, K.-S., Ryu, P.-M., Chen, H.-H., Donatelli, L., Ji, H., Kurohashi, S., Paggio, P., Xue, N., Kim, S., Hahm, Y., He, Z., Lee, T. K., Santus, E., Bond, F., and Na, S.-H. (eds.), *Proceedings of the 29th International Conference on Computational Linguistics*, pp. 1511–1520, Gyeongju, Republic of Korea, October 2022. International Committee on Computational Linguistics. URL <https://aclanthology.org/2022.coling-1.130/>.

Chen, J., Li, T., Qin, J., Lu, P., Lin, L., Chen, C., and Liang, X. Unigeo: Unifying geometry logical reasoning via reformulating mathematical expression. *arXiv preprint arXiv:2212.02746*, 2022.

Chen, L., Li, J., Dong, X., Zhang, P., Zang, Y., Chen, Z., Duan, H., Wang, J., Qiao, Y., Lin, D., et al. Are we on the right way for evaluating large vision-language models? *Advances in Neural Information Processing Systems*, 37: 27056–27087, 2024a.

Chen, X., Hu, W., Li, H., Zhou, J., Chen, Z., Cao, M., Zeng, Y., Zhang, K., Yuan, Y.-J., Han, J., et al. C2-evo: Co-evolving multimodal data and model for self-improving reasoning. *arXiv preprint arXiv:2507.16518*, 2025a.

Chen, X., Lu, J., Kim, M., Zhang, D., Tang, J., Piché, A., Gontier, N., Bengio, Y., and Kamalloo, E. Self-evolving curriculum for llm reasoning. *arXiv preprint arXiv:2505.14970*, 2025b.

Chen, Z., Deng, Y., Yuan, H., Ji, K., and Gu, Q. Self-play fine-tuning converts weak language models to strong language models. *arXiv preprint arXiv:2401.01335*, 2024b.

Douze, M., Guzhva, A., Deng, C., Johnson, J., Szilvassy, G., Mazaré, P.-E., Lomeli, M., Hosseini, L., and Jégou, H. The faiss library. *IEEE Transactions on Big Data*, 2025.

Fang, W., Liu, S., Zhou, Y., Zhang, K., Zheng, T., Chen, K., Song, M., and Tao, D. Serl: Self-play reinforcement learning for large language models with limited data. *arXiv preprint arXiv:2505.20347*, 2025.

Gao, H.-a., Geng, J., Hua, W., Hu, M., Juan, X., Liu, H., Liu, S., Qiu, J., Qi, X., Wu, Y., et al. A survey of self-evolving agents: On path to artificial super intelligence. *arXiv preprint arXiv:2507.21046*, 2025.

Guan, T., Liu, F., Wu, X., Xian, R., Li, Z., Liu, X., Wang, X., Chen, L., Huang, F., Yacoob, Y., et al. Hallusionbench: an advanced diagnostic suite for entangled language hallucination and visual illusion in large vision-language models. In *Proceedings of the IEEE/CVF Conference on Computer Vision and Pattern Recognition*, pp. 14375–14385, 2024.

He, Y., Huang, C., Li, Z., Huang, J., and Yang, Y. Visplay: Self-evolving vision-language models from images. *arXiv preprint arXiv:2511.15661*, 2025.

Huang, C., Yu, W., Wang, X., Zhang, H., Li, Z., Li, R., Huang, J., Mi, H., and Yu, D. R-zero: Self-evolving reasoning llm from zero data. *arXiv preprint arXiv:2508.05004*, 2025.

Lambert, N., Morrison, J., Pyatkin, V., Huang, S., Ivison, H., Brahman, F., Miranda, L. J. V., Liu, A., Dziri, N., Lyu, S., et al. Tulu 3: Pushing frontiers in open language model post-training. *arXiv preprint arXiv:2411.15124*, 2024.

Laurençon, H., Tronchon, L., Cord, M., and Sanh, V. What matters when building vision-language models?, 2024.

Liu, A., Mei, A., Lin, B., Xue, B., Wang, B., Xu, B., Wu, B., Zhang, B., Lin, C., Dong, C., et al. Deepseek-v3. 2: Pushing the frontier of open large language models. *arXiv preprint arXiv:2512.02556*, 2025a.

Liu, B., Jin, C., Kim, S., Yuan, W., Zhao, W., Kulikov, I., Li, X., Sukhbaatar, S., Lanchantin, J., and Weston, J. Spice: Self-play in corpus environments improves reasoning. *arXiv preprint arXiv:2510.24684*, 2025b.

Lu, P., Gong, R., Jiang, S., Qiu, L., Huang, S., Liang, X., and Zhu, S.-C. Inter-gps: Interpretable geometry problem solving with formal language and symbolic reasoning. *arXiv preprint arXiv:2105.04165*, 2021.

Lu, P., Bansal, H., Xia, T., Liu, J., Li, C., Hajishirzi, H., Cheng, H., Chang, K.-W., Galley, M., and Gao, J. Mathvista: Evaluating mathematical reasoning of foundation models in visual contexts. *arXiv preprint arXiv:2310.02255*, 2023.

Qiao, R., Tan, Q., Dong, G., MinhuiWu, M., Sun, C., Song, X., Wang, J., Gongque, Z., Lei, S., Zhang, Y., et al. We-math: Does your large multimodal model achieve human-like mathematical reasoning? In *Proceedings of the 63rd Annual Meeting of the Association for Computational Linguistics (Volume 1: Long Papers)*, pp. 20023–20070, 2025.

Radford, A., Kim, J. W., Hallacy, C., Ramesh, A., Goh, G., Agarwal, S., Sastry, G., Askell, A., Mishkin, P., Clark, J., et al. Learning transferable visual models from natural language supervision. In *International conference on machine learning*, pp. 8748–8763. PMLR, 2021.

Safaei, B. and Patel, V. M. Active learning for vision-language models. In *2025 IEEE/CVF Winter Conference on Applications of Computer Vision (WACV)*, pp. 4902–4912. IEEE, 2025.

Shao, Z., Wang, P., Zhu, Q., Xu, R., Song, J., Bi, X., Zhang, H., Zhang, M., Li, Y., Wu, Y., et al. Deepseekmath: Pushing the limits of mathematical reasoning in open language models. *arXiv preprint arXiv:2402.03300*, 2024.

Silver, D., Hubert, T., Schrittwieser, J., Antonoglou, I., Lai, M., Guez, A., Lanctot, M., Sifre, L., Kumaran, D., Graepel, T., et al. A general reinforcement learning algorithm that masters chess, shogi, and go through self-play. *Science*, 362(6419):1140–1144, 2018.

Thawakar, O., Venkatraman, S., Thawkar, R., Shaker, A., Cholakkal, H., Anwer, R. M., Khan, S., and Khan, F. Evolmm: Self-evolving large multimodal models with continuous rewards. *arXiv preprint arXiv:2511.16672*, 2025.

Tschannen, M., Gritsenko, A., Wang, X., Naeem, M. F., Alabdulmohsin, I., Parthasarathy, N., Evans, T., Beyer, L., Xia, Y., Mustafa, B., et al. Siglip 2: Multilingual vision-language encoders with improved semantic understanding, localization, and dense features. *arXiv preprint arXiv:2502.14786*, 2025.

Udandarao, V., Parthasarathy, N., Naeem, M. F., Evans, T., Albanie, S., Tombari, F., Xian, Y., Tonioni, A., and Hénaff, O. J. Active data curation effectively distills large-scale multimodal models. In *Proceedings of the Computer Vision and Pattern Recognition Conference*, pp. 14422–14437, 2025.

Wang, K., Pan, J., Shi, W., Lu, Z., Ren, H., Zhou, A., Zhan, M., and Li, H. Measuring multimodal mathematical reasoning with math-vision dataset. *Advances in Neural Information Processing Systems*, 37:95095–95169, 2024.

Wang, Q., Liu, B., Zhou, T., Shi, J., Lin, Y., Chen, Y., Li, H. H., Wan, K., and Zhao, W. Vision-zero: Scalable vlm self-improvement via strategic gamified self-play. *arXiv preprint arXiv:2509.25541*, 2025a.

Wang, Z., Guo, X., Stoica, S., Xu, H., Wang, H., Ha, H., Chen, X., Chen, Y., Yan, M., Huang, F., et al. Perception-aware policy optimization for multimodal reasoning. *arXiv preprint arXiv:2507.06448*, 2025b.

Weng, T., Wang, J., Jiang, W., and Ming, Z. Visnumbench: Evaluating number sense of multimodal large language models. *arXiv preprint arXiv:2503.14939*, 2025.

Wu, Y., Sun, Z., Yuan, H., Ji, K., Yang, Y., and Gu, Q. Self-play preference optimization for language model alignment. *arXiv preprint arXiv:2405.00675*, 2024.

xAI. Grok-1.5 vision preview, April 2024. URL <https://x.ai/news/grok-1.5v>. Introduces the Real-WorldQA benchmark and dataset (accessed 2026-01-28).

Xiao, Y., Sun, E., Liu, T., and Wang, W. Logicvista: Multimodal llm logical reasoning benchmark in visual contexts. *arXiv preprint arXiv:2407.04973*, 2024.

Yang, Z., Shen, W., Li, C., Chen, R., Wan, F., Yan, M., Quan, X., and Huang, F. Spell: Self-play reinforcement learning for evolving long-context language models. *arXiv preprint arXiv:2509.23863*, 2025.

Yue, X., Ni, Y., Zhang, K., Zheng, T., Liu, R., Zhang, G., Stevens, S., Jiang, D., Ren, W., Sun, Y., et al. Mmmu: A

massive multi-discipline multimodal understanding and reasoning benchmark for expert agi. In *Proceedings of the IEEE/CVF Conference on Computer Vision and Pattern Recognition*, pp. 9556–9567, 2024.

Yue, X., Zheng, T., Ni, Y., Wang, Y., Zhang, K., Tong, S., Sun, Y., Yu, B., Zhang, G., Sun, H., et al. Mmmu-pro: A more robust multi-discipline multimodal understanding benchmark. In *Proceedings of the 63rd Annual Meeting of the Association for Computational Linguistics (Volume 1: Long Papers)*, pp. 15134–15186, 2025.

Zhang, R., Jiang, D., Zhang, Y., Lin, H., Guo, Z., Qiu, P., Zhou, A., Lu, P., Chang, K.-W., Qiao, Y., et al. Mathverse: Does your multi-modal lilm truly see the diagrams in visual math problems? In *European Conference on Computer Vision*, pp. 169–186. Springer, 2024.

Zhang, X., Liangyu, X., Duan, F., Zhou, Y., Wang, S., Weng, R., Wang, J., and Cai, X. Preference curriculum: Llms should always be pretrained on their preferred data. In *Findings of the Association for Computational Linguistics: ACL 2025*, pp. 21181–21198, 2025.

Zhao, A., Wu, Y., Yue, Y., Wu, T., Xu, Q., Lin, M., Wang, S., Wu, Q., Zheng, Z., and Huang, G. Absolute zero: Reinforced self-play reasoning with zero data. *arXiv preprint arXiv:2505.03335*, 2025.

Zheng, Y., Lu, J., Wang, S., Feng, Z., Kuang, D., and Xiong, Y. Easyr1: An efficient, scalable, multi-modality rl training framework. <https://github.com/hiyouga/EasyR1>, 2025.

Zou, C., Guo, X., Yang, R., Zhang, J., Hu, B., and Zhang, H. Dynamath: A dynamic visual benchmark for evaluating mathematical reasoning robustness of vision language models. *arXiv preprint arXiv:2411.00836*, 2024.

A. Experiment Setup

A.1. Evaluation Benchmarks.

We evaluate models on two groups of benchmarks: (i) reasoning-intensive visual math/logic suites and (ii) general visual understanding + knowledge suites. Below we introduce each benchmark in the order shown in our tables.

- **MathVista** (Lu et al., 2023) is a consolidated benchmark for mathematical reasoning in a visual context. It aggregates problems from many prior multimodal math datasets and also includes newly created subsets, targeting fine-grained perception (reading plots/diagrams/tables) and multi-step reasoning. Evaluation is conducted on testmini split, with 1,000 samples.
- **MathVision (MATH-Vision)** (Wang et al., 2024) is a curated set of competition-style math problems with visual context, designed to expand subject coverage and difficulty beyond earlier visual-math benchmarks. It spans multiple math disciplines and difficulty levels to stress robust multimodal math reasoning. Evaluation is conducted on the test split, with 3,040 samples.
- **WeMath (WE-MATH)** (Qiao et al., 2025) focuses on process-level visual mathematical reasoning. Besides end accuracy, it emphasizes diagnosing how models solve problems by organizing questions along hierarchical knowledge concepts and finer-grained skill layers. Evaluation is conducted on the testmini split, with 1,740 samples.
- **MathVerse** (Zhang et al., 2024) is a holistic visual-math benchmark with curated diagram-based problems. A key feature is that each problem can be presented in multiple “versions” with different modality/information availability, enabling controlled analysis of whether models truly use the diagram and how multimodal information contributes to solving. We use the Vision Dominant + Vision Intensive variants filtered from the testmini split, comprising 1,576 samples, which emphasize solving with strong dependence on the image content.
- **LogicVista** (Xiao et al., 2024) targets general logical reasoning in visual contexts (beyond math), with multiple-choice annotated questions spanning several categories of reasoning skills (e.g., inductive/deductive/spatial/numerical/mechanical-style reasoning). Evaluation is conducted on the test split, with 448 samples.
- **DynaMath** (Zou et al., 2024) evaluates robustness in multimodal mathematical reasoning under dynamic visual/textual variations. It represents seed questions as programs to automatically generate diverse instantiations, testing stability under perturbations rather than performance on a single static set. Evaluation is conducted on all splits, with 5,010 samples.
- **VisNum (VisNumBench)** (Weng et al., 2025) measures visual number sense: estimating/counting/comparing quantities and other numerical attributes from images, using both synthetic and real-world scenarios to probe how well models ground numeric reasoning in perception. Evaluation is conducted on the test split, with 1,913 samples.
- **RealWorld (RealWorldQA)** (xAI, 2024) is designed to test basic real-world spatial understanding from everyday photos (e.g., relative positions, simple spatial relations) with straightforward, verifiable answers—often easy for humans but challenging for models. Evaluation is conducted on the test split, with 765 samples.
- **MMStar** (Chen et al., 2024a) is an elite vision-indispensable multimodal benchmark built via careful human selection to reduce spurious shortcuts and ensure visual dependency. It evaluates multiple core capability axes and is commonly used as a general diagnostic of LVLM multimodal competence. Evaluation is conducted on the val split, with 1,500 samples.
- **MMMU** (Yue et al., 2024) is a large-scale, multi-discipline benchmark drawn from college-level exams/quizzes/textbooks, requiring subject knowledge and deliberate reasoning over diverse visual formats (e.g., diagrams, tables, charts). It is widely used to assess knowledge-intensive multimodal understanding. Evaluation is conducted on the test set with 895 samples.
- **MMMU_Pro** (Yue et al., 2025) is a more robust variant of MMMU designed to better isolate genuine multimodal understanding (e.g., reducing text-only solvable items and strengthening evaluation settings so models must integrate vision and text). We use the standard (4 options) test split (filtered to single-image questions), comprising 1,591 samples.
- **Hallusion (HallusionBench)** (Guan et al., 2024) evaluates hallucination and visual illusion failures in vision-language models via expert-written question sets with control-style structure, stressing consistency and grounded image-context reasoning beyond simple object hallucination checks. Evaluation is conducted on the test split, with 951 samples.

A.2. Implementation Details

In our iterative self-play setup, we conduct three full cycles. Within each iteration, we train the Searcher and Questioner for 10 optimization steps and the Solver for 30 optimization steps. We report results from the second iteration, which yields the best performance. We use a batch size of 512 with a PPO minibatch size of 128. The sampling temperature is 1.0, and the maximum generation length is 2048 tokens. To produce reliable pseudo-labels, we sample $K = 9$ trajectories and apply majority voting. To compute uncertainty-based rewards for the Searcher and Questioner, we perform $m = 10$ rollouts.

A.3. Models and baselines

As the foundational backbone of our framework, we employ the Qwen2.5-VL series (Bai et al., 2025), specifically the 3B-Instruct and 7B-Instruct variants. For baselines, we compare with recent self-play methods developed for VLMs. For VisPlay (He et al., 2025), we reproduce the results closely following the official open-source repository and the training procedures provided by the authors. For Vision-Zero (Wang et al., 2025a) and EvoLMM (Thawakar et al., 2025), we directly evaluate the publicly released model weights.

B. Prompt Templates

Solver Prompt Template

Please reason step by step carefully based on the question: {question} and the image. After completing your reasoning, you MUST output the final, clean, and concise answer strictly inside \boxed{{}}. The final answer MUST appear inside \boxed{{}}, and nowhere else. If there is no boxed answer, your response is considered incorrect.

Searcher Prompt Template

You are an AI Data Engineer. Your task is to generate a unique and concise image retrieval query.

Target Category: {category}

Focus on: {query sample}

Diversity Requirements:

Vary the Subject: Do not use common examples. Explore different specific objects within the focus area.

Output Format:

```
<type>{category}</type>
<query>[Concise description emphasizing structure and key markers based on the
focus keywords]</query>
```

Example (Reference only, DO NOT COPY):

```
<type>{category}</type>
<query>{query sample}</query>
```

LLM Judge Prompt Template

System Message:

You are an answer evaluation assistant. Your task is to judge whether two answers are substantially equivalent. When evaluating, you should ignore superficial differences such as format, spaces, punctuation, case, etc., and focus on whether they are consistent in core content, logical meaning and information expression. The judgment criteria should be lenient and inclusive, as long as the expressed meaning is basically the same, it is considered equivalent.

User Message:

Given the question {question}, please judge whether the following two answers express the same meaning. Please only answer "correct" or "incorrect". Correct answer: {ground_truth_answer}. Answer to be judged: {predicted_answer}. Judgment result (only answer "correct" or "incorrect"). You don't need to reason, just answer "correct" or "incorrect". Don't say anything else. Only answer "correct" or "incorrect" directly without thinking.

Questioner Prompt Template

You are an Expert Visual Reasoning Specialist. Your task is to analyze the image, identify core constraints, and generate a high-quality reasoning question that requires multi-step derivation.

Requirements:

- The **Analysis Phase** must contain:
 - **Visible Elements:** List specific labels, numbers, objects, and spatial markers.
 - **Constraints:** Identify explicit or implicit rules (e.g., parallel lines, gravity, total percentages in a chart).
 - **Step-by-Step Solution:** Solve your intended question entirely using only the image data to ensure it is mathematically/logically sound.
- **No Simple Description:** Do NOT ask questions that can be answered by simple object identification, color naming, or simple counting.
- **Logical Depth:** The question must require interpreting intent, calculating based on visual cues, spatial transformations, or inferring cause-and-effect.

Question Type:

1. `short_answer`: Requires a short phrase based on logical inference.
2. `numeric_value`: Requires a calculation or estimation. Provide only the pure number.

Output Format:

```
<think>A</think>
<type>X</type>
<question>Y</question>
<answer>Z</answer>
```

Strict Rules:

- A must be the analysis phase.
- X must be one of: `short_answer` or `numeric_value`.
- Z must be the minimal correct value (phrase or number).
- Do not add any extra text, labels, or explanations.

Examples of Reasoning-based Questions:

<think>Visible Elements: A balanced scale shows 3 circles on the left and 2 squares on the right. Constraints: Balanced means equal total weight. Step-by-Step Solution: $3c = 2s \Rightarrow s = 1.5c$, so a square is heavier than a circle.</think>

```
<type>short_answer</type>
<question>Which is heavier: one square or one circle?</question>
<answer>square</answer>
```

<think>Visible Elements: A triangle with base labeled y, left side labeled 12, right side labeled x, base angles labeled 30° (left) and 60° (right), and a right-angle marker at the top indicating 90° . Constraints: A 30° - 60° - 90° triangle has side ratios $1 : \sqrt{3} : 2$ (opposite 30° , 60° , 90° respectively). Step-by-Step Solution: The side 12 is opposite 60° , so $12 = \sqrt{3}k \Rightarrow k = \frac{12}{\sqrt{3}} = 4\sqrt{3}$. The hypotenuse is $y = 2k = 8\sqrt{3}$.</think>

```
<type>numeric_value</type>
<question>Find y.</question>
<answer>8\sqrt{3}</answer>
```

Table 4. Comparison of **Active-Zero** against state-of-the-art baselines on reasoning-intensive benchmarks.

Method	MathVista	MathVision	WeMath	MathVerse	LogicVista	DynaMath	Average
<i>Qwen2.5-VL-3B-Instruct</i>							
Base Model	57.80	22.27	53.51	30.84	37.28	46.33	41.34
Active-Zero (Iter1)	59.20	23.06	60.06	33.88	39.96	50.30	44.41
Active-Zero (Iter2)	60.20	23.62	61.21	35.09	40.62	51.24	45.33
Active-Zero (Iter3)	59.00	22.20	61.09	33.88	40.40	51.00	44.60
<i>Qwen2.5-VL-7B-Instruct</i>							
Base Model	69.40	25.95	64.48	45.11	43.08	58.26	51.05
Active-Zero (Iter1)	71.60	26.97	68.16	46.76	46.21	59.54	53.21
Active-Zero (Iter2)	72.60	26.18	69.60	48.16	48.21	59.04	53.97
Active-Zero (Iter3)	72.30	26.61	69.94	45.88	47.54	58.52	53.47

 Table 5. Comparison of **Active-Zero** against state-of-the-art baselines on general visual understanding and knowledge-based benchmarks.

Method	VisNum	RealWorld	MMStar	MMMU	MMMU_Pro	Hallusion	Average
<i>Qwen2.5-VL-3B-Instruct</i>							
Base Model	34.71	61.70	52.80	44.69	41.99	60.04	49.32
Active-Zero (Iter1)	40.93	61.44	53.20	47.93	46.64	64.25	52.40
Active-Zero (Iter2)	41.51	60.00	53.80	49.16	46.70	64.14	52.55
Active-Zero (Iter3)	41.51	60.26	52.80	48.27	45.69	63.72	52.04
<i>Qwen2.5-VL-7B-Instruct</i>							
Base Model	44.85	63.66	61.53	53.52	52.61	68.87	57.51
Active-Zero (Iter1)	45.53	66.01	62.40	54.30	53.30	69.61	58.53
Active-Zero (Iter2)	47.94	67.58	64.00	56.42	54.62	68.03	59.77
Active-Zero (Iter3)	48.35	67.45	64.33	54.75	51.60	69.51	59.33

C. Detailed Results

Table 4 and Table 5 present a comprehensive comparison of **Active-Zero** against strong baselines across both reasoning-intensive and general visual understanding benchmarks, evaluated at two model scales (Qwen2.5-VL-3B-Instruct and Qwen2.5-VL-7B-Instruct) and over multiple self-play iterations.

Reasoning-Intensive Benchmarks On reasoning-intensive tasks, **Active-Zero** consistently improves performance over the base model across all six benchmarks and both model sizes, demonstrating the effectiveness and robustness of the proposed training strategy. For Qwen2.5-VL-3B-Instruct, the base model achieves an average score of 41.34. After applying **Active-Zero**, performance increases substantially, peaking at 45.33 (+3.99) in Iter2. Gains are broad and systematic: MathVista (+2.40), WeMath (+7.70), MathVerse (+4.25), LogicVista (+3.34), and DynaMath (+4.91) all see notable improvements. Iter3 shows a slight regression relative to Iter2, suggesting diminishing returns or mild overfitting with continued iterations at this scale. For Qwen2.5-VL-7B-Instruct, **Active-Zero** yields great and stable improvements. The average score increases from 51.05 (base) to 53.97 (+2.92) at Iter2, with Iter3 remaining competitive at 53.47. The most pronounced gains are observed on LogicVista (43.08 → 48.21, +5.13) and WeMath (64.48 → 69.60, +5.12), highlighting **Active-Zero**'s effectiveness on benchmarks that require multi-step logical reasoning and mathematical abstraction. Improvements are also consistent on MathVista, MathVision, and MathVerse, indicating that the method generalizes across diverse reasoning formats rather than targeting a narrow task type. Overall, these results show that **Active-Zero** not only improves average performance but does so uniformly across benchmarks, reinforcing its advantage over static or manually designed curricula.

General Visual Understanding and Knowledge-Based Benchmarks

Table 5 examines whether improvements on reasoning-intensive tasks trade off against general visual understanding or factual knowledge. Overall, **Active-Zero** preserves—and often strengthens—performance on these complementary benchmarks. For Qwen2.5-VL-3B-Instruct, the average score rises from 49.32 to 52.55 (+3.23) at Iter2. The largest gains come from VisNum (+6.80), MMMU (+4.47), and MMMU_Pro (+4.71), indicating better numerical and multidisciplinary reasoning. While RealWorld drops slightly compared to the base model, improvements on the remaining benchmarks more than offset

Table 6. Ablation Study of **Active-Zero** on reasoning-intensive benchmarks.

Method	MathVista	MathVision	WeMath	MathVerse	LogicVista	DynaMath	Average
<i>Qwen2.5-VL-3B-Instruct</i>							
Base Model	57.80	22.27	53.51	30.84	37.28	46.33	41.34
Active-Zero	60.20	23.62	61.21	35.09	40.62	51.24	45.33
Base Challenger	59.30	21.88	61.32	34.39	40.40	51.18	44.75
Random Sampling	58.60	23.16	56.72	34.96	39.06	50.80	43.88
w/o Domain-Condition	59.20	22.43	62.41	35.15	39.73	50.68	44.93
w/o Visual Penalty	59.40	22.20	62.24	33.88	40.18	50.72	44.89

 Table 7. Ablation Study of **Active-Zero** on general visual understanding and knowledge-based benchmarks.

Method	VisNum	RealWorld	MMStar	MMMU	MMMU_Pro	Hallusion	Average
<i>Qwen2.5-VL-3B-Instruct</i>							
Base Model	34.71	61.70	52.80	44.69	41.99	60.04	49.32
Active-Zero	41.51	60.00	53.80	49.16	46.70	64.14	52.55
Base Challenger	40.51	57.91	52.53	47.37	44.75	63.09	51.03
Random Sampling	37.69	63.53	53.27	47.82	44.06	64.77	51.86
w/o Domain-Condition	40.04	57.39	52.20	47.71	45.13	61.93	50.73
w/o Visual Penalty	41.82	59.61	54.13	47.15	44.88	62.15	51.62

this decline, yielding a clear net gain. For Qwen2.5-VL-7B-Instruct, **Active-Zero** increases the average from 57.51 to 59.77 (+2.26) at Iter2, with the most pronounced gains on RealWorld (+3.92), VisNum (+3.09), and MMMU (+2.90). Although Iter3 shows mild regressions on MMMU_Pro and Hallusion relative to Iter2, results remain consistently above the base model, suggesting that additional iterations do not meaningfully erode general capabilities.

Iterative Behavior and Scaling Trends

Across both tables, Iter2 consistently emerges as the strongest iteration, striking a balance between exploration and stability. Iter3 often yields marginal regressions, particularly on smaller models, suggesting that excessive self-play iterations may introduce noise or reduce data diversity. Importantly, the gains from **Active-Zero** persist and scale well from 3B to 7B models, demonstrating that the method is not tied to a specific model capacity.